WEP Warwick Evans Publishing

International Journal of Mechanical and Electrical Engineering

ISSN: 3005-9615 (Print), ISSN: 3005-7132 (Online) | Volume 8, Number 1, Year 2026
DOI: https://doi.org/10.62051/ijmee.v8n1.06
Journal homepage: https://wepub.org/index.php/IJMEE/index

Research on Strawberry Quality Inspection Based on Hyperspectral Imaging Technology

Shu Jiang, Jianwen Jiang

College of Electrical and Automation Engineering, East China Jiaotong University, Nanchang, Jiangxi, China

ABSTRACT

This study integrates hyper-spectral imaging technology, data mining, and image processing to explore its application in non-destructive quality assessment of strawberries, including evaluations of appearance, maturity, and internal quality. It also investigates the impact of different feature selection algorithms on classification accuracy. The research contributes to the development of automated quality grading systems for off-season strawberries, reducing post-harvest losses and enhancing fruit quality. Key findings include: (1) Analysis of strawberry quality parameters and spectral characteristics changes (2) High-spectral imaging-based strawberry hardness detection method (3) Detection of Soluble Solid Content (SSC) in Strawberries Using Hyper-spectral Imaging

KEYWORDS

Hyper-spectral Technology; Cherry strawberry; Soluble Solid Content; Hardness Quality Detection.

1. INTRODUCTION

Strawberries belong to the Rosaceae family and rank first in the global production of small berries. Renowned for their soft, juicy texture and rich nutritional content, strawberries contain 50-100 milligrams of vitamin C per 100 grams—more than ten times the amount found in apples and grapes—earning them the reputation of the "Queen of Fruits". As the world's largest producer and consumer of strawberries, China accounts for over one-third of the global annual output.The external color and the content of soluble solids in strawberries are two crucial indicators for evaluating strawberry quality. Traditional physical and chemical methods involve measuring soluble solids with a handheld refractometer and determining acidity via titration. Although these conventional approaches yield relatively accurate results, they are time-consuming, labor-intensive, and destructive to the fruit. Thus, neither method is suitable for the rapid and non-destructive testing of strawberries [5-6]. With their thin skins and short shelf lives, strawberries are highly susceptible to damage. The drawbacks of traditional methods, such as destructiveness, cumbersome operations, and stringent experimental conditions, have severely hindered the development of the fruit industry.

In contrast to traditional quality testing methods, non-destructive testing (NDT) techniques offer advantages of speed, non-invasiveness, and high precision. They enable real-time analysis of internal quality while preserving the fruit's integrity, which is of great significance for the advancement of China's fruit industry [7].In recent years, non-destructive testing technologies such as hyperspectral imaging, computer vision, and information fusion have been widely applied and rapidly developed in fruit quality assessment [8-10]. The greatest merit of NDT techniques is that they do not require direct contact with the tested object, thereby avoiding secondary damage. By leveraging the response changes of the object’s internal chemical components and external characteristics to light, electricity, magnetism, and other stimuli, these techniques can detect both internal chemical compositions and

external traits.Developing a rapid, accurate, and efficient method for strawberry quality testing is therefore imperative, as it plays a vital role in improving fruit quality and enhancing market competitiveness.

2. EXPERIMENTAL DATA AND ANALYSIS METHODS

Using strawberries as the experimental samples, hyperspectral image information and hardness data were collected within the wavelength range of 400nm to 1000nm. Preliminary experiments showed that strawberries stored at room temperature would show visible mold within 3 days, so this experiment only collected spectral data for strawberries over 3 days. The experimental samples were fresh strawberries from a certain strawberry farm, with a total of 200 strawberries harvested. They were sent to the laboratory within three hours after picking, and data collection experiments were conducted in the afternoon, with the same experiment repeated every 24 hours, completing three days of data collection. After removing moldy and damaged strawberries, spectral images and hardness data of 166 strawberries were finally retained.

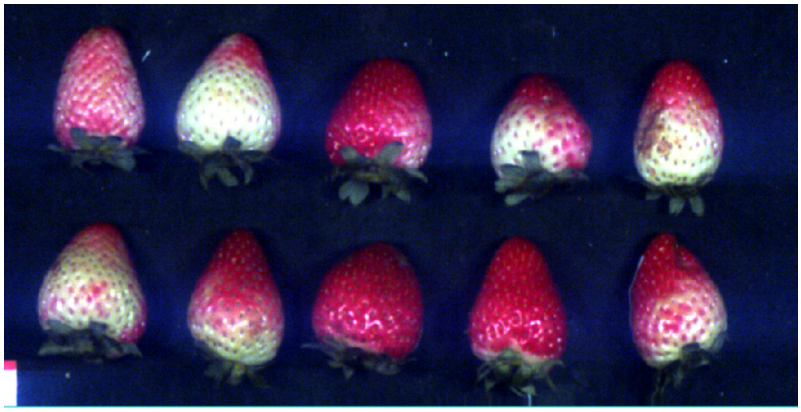

Figure 1. Strawberry sample image

2.1. Data acquisition

The hyper-spectral reflectance imaging system (hyperspectral imager) will be used to acquire hyperspectral images of all strawberry samples. The system has a spectral range of 400-1000 nm and a spectral resolution of 2.31 nm. The imaging system consists of a hyperspectral spectrometer, a CCD camera with a resolution of 696×696, two tungsten-halogen lamps with a wavelength range of 300–2500 nm, a moving platform, a dark box, and a computer equipped with hyperspectral image acquisition software Hyper-scanner [27,28], as shown in Figure 2.

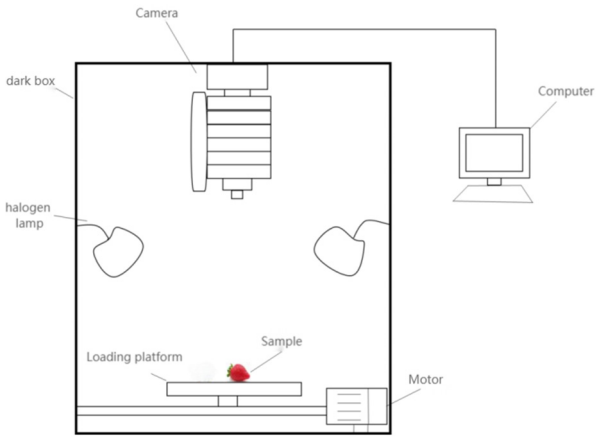

Figure 2. Visible-Near Infrared Hyper-spectral Imaging System

After the hyperspectral image acquisition is completed, the strawberry samples need to be immediately removed to minimize thermal damage from the tungsten halogen lamp. Due to interference from external factors such as uneven light distribution and camera dark current, the acquired hyperspectral images need to be corrected [19]. The correction formula is as follows:

$$R=\frac{R_{raw}-R_d}{R_w-R_d} \quad (1)$$

Here, R is the corrected hyperspectral image, Rraw is the original hyperspectral image, Rw is the white reference image obtained from a whiteboard with 99% reflectance, and Rd is the black reference image obtained by turning off the lights and covering the camera lens. The corrected hyperspectral image will be used for subsequent analysis.

After acquiring the hyperspectral image data, it is necessary to extract the spectral characteristics of the strawberries in the hyperspectral images. Since the hyperspectral images collected in the experiment contain backgrounds unrelated to the objects being detected, the strawberry regions in the images must first be selected. Removing these backgrounds and selecting the study area is also known as Region of Interest (ROI) extraction [16]. There are generally two methods for extracting an ROI: one is to extract the ROI through image segmentation techniques; the other is to use relevant specialized software, such as ENVI, to directly select the desired area and then treat that area as the ROI. This paper will use the second method to extract the ROI. After ROI extraction, the spectra of all pixels within this area can be extracted for subsequent analysis.

2.2. Analytical Method

Visible/near-infrared spectral analysis technology is a rapid, multifunctional, and non-destructive detection method that has been widely used in industrial production, food safety, and environmental protection. This study utilizes visible/near-infrared spectroscopy to analyze and detect the quality of strawberries. Specifically, visible light has a wavelength range of 380 to 780 nm, while near-infrared lies between visible and mid-infrared, ranging from 780 to 1100 nm. Almost all organic structures and functional groups can be identified using visible/near-infrared spectroscopy. When the light source illuminates the surface of a strawberry, phenomena such as reflection, absorption, transmission, and diffuse reflection occur. Due to changes in scattering and absorption processes, the spectral characteristics of the incident light change as it penetrates the strawberry. The light scattering properties of strawberries are closely related to their chemical composition and microstructure. There are various organic molecules in strawberries that can selectively absorb photons, triggering optical reactions and thereby altering the characteristics of visible/near-infrared light.

Convolutional Neural Networks (CNNs) are a type of deep feedforward neural network specifically designed to process grid-structured data and are one of the key algorithms in deep learning. Their core features include local connectivity and weight sharing, which enable outstanding performance in computer vision tasks, and they are widely used in image classification, object detection, and semantic segmentation. CNNs mainly consist of convolutional layers, activation functions, pooling layers, fully connected layers, and output layers, possessing strong representation learning capabilities, able to automatically extract features and efficiently represent complex patterns through a hierarchical structure.

2.3. Modeling Method

SVM models are commonly used to simplify complex learning processes by simulating nonlinear behaviors and obtaining necessary information to make appropriate decisions. In other words, in predictive problems involving uncertainties in various aspects, SVM models are a powerful approach. Their characteristics include control of the decision function's capacity, the use of kernel functions, and sparsity of the solution. SVM, based on the unique theory of the structural risk minimization

principle, estimates functions by minimizing the upper bound of the generalization error, therefore it is highly resistant to overfitting and ultimately achieves good generalization performance.

PLSR is a statistical algorithm that is somewhat related to principal component regression. It establishes a linear regression model by projecting both the dependent and independent variables into another common space. The PLSR model is also referred to as a bilinear factor model. More specifically, the PLSR method can analyze the information shared by the X and Y matrices, that is, it builds a latent variable model of the covariance structure in these two spaces [31].

3. RESULTS AND DISCUSSION

3.1. Strawberry Quality Parameters

The quality parameters of strawberries do not change independently; they are interconnected and influence each other. To reveal this internal relationship, a correlation analysis was conducted on three key quality indicators: hardness, SSC, and weight loss rate (Table 1).

Table 1. Correlation matrix of strawberry quality parameters (n=300)

Quality parameters	Hardness(N)	SSC	Weightlessness rate(%)
Hardness	1.00	0.58**	-0.82**
SSC	0.58**	1.00	-0.47**
Weightlessness rate	-0.82**	-0.47**	1.00

Note: **Indicates a significant correlation at the P<0.01 level

Key findings:

1. Hardness was significantly negatively correlated with weight loss rate (r=-0.82, P<0.01), indicating that water loss was one of the main reasons for strawberry softening. For every 1% increase in weight loss rate, the hardness decreases by about 0.28N.

2. Hardness was moderately positively correlated with SSC (r=0.58, P<0.01), indicating that the texture was usually maintained in the early stage of sugar accumulation, but the relationship between the two weakened after over-maturation.

3. SSC was negatively correlated with weight loss rate (r=-0.47, P<0.01), but the correlation was weak, indicating that SSC changes were not entirely caused by water evaporation, and material transformation also played an important role.

After systematically analyzing the changes of quality parameters and their relationship with hyperspectral characteristics during the storage period of 3-5 days, the main conclusions are as follows:

1. The weight loss rate increased linearly from 0% to 8.73%, and the average daily weight loss rate was about 1.75%, which was mainly controlled by water evaporation.

2. SSC showed a trend of first rising and then decreasing, peaking on day 2 (9.16°Brix) and decreasing due to respiratory expenditure in the later stage.

3. The hardness continued to decrease from 4.56N to 2.13N, a decrease of 53.3%, and the softening mainly occurred in the early stage of storage.

4. There was a significant correlation between various quality parameters, especially the hardness was highly negatively correlated with the weight loss rate (r=-0.82).

5. Visible light region (400-700 nm): The reflectivity of the 550 nm green peak increases, and the chlorophyll absorption valley becomes lighter at 670 nm, reflecting pigment degradation.

6. Red-edged area (700-750 nm): The red-edged area is blue-shifted, and the reflectivity decreases, which is a sensitive indicator of mature aging.

7. Near-infrared region (750-1000 nm): The decrease in reflectance at 850 nm reflects the disruption of cellular structure, and the shallow water absorption valley at 960 nm indicates water loss.

3.2. Strawberry Hardness Test

Through preliminary experiments, it was found that strawberries show visible mold after being stored at room temperature for 3 days. Therefore, this experiment only collected spectral data of strawberries for 3 days. After removing moldy and damaged strawberries, a total of 166 strawberries' spectral images and hardness data were retained.

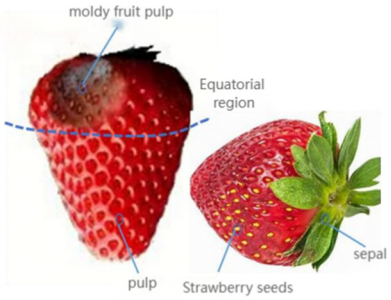

Figure 3. Different components of strawberries

SVM and RF were used to establish a classification model for strawberry storage time, while PLSR, SVM, and RF were used to establish a predictive regression model for strawberry storage time. Among 200 strawberry samples, 120 samples were first selected and divided into two groups. According to the Kennard-Stone algorithm, 80 samples were chosen as the calibration set to build the model, and the remaining 40 samples served as the prediction set to evaluate the model's performance. The performance of the classification model was assessed using the calibration set accuracy (ACCC) and prediction set accuracy (ACCp). The performance of the regression model was evaluated using the coefficient of determination for the calibration set (Rc^2) and prediction set (Rp^2), as well as the root mean square error of the calibration set (RMSEC) and prediction set (RMSEP).

Here, the closer the correlation coefficient is to 1, the better the training and prediction performance. CCCS and CCPS < 0.3 indicate weak correlation, 0.3–0.5 indicates moderate correlation, and greater than 0.5 indicates strong correlation. The closer the root mean square error is to 0, the closer the model's predictions are to the true values. A larger RPD indicates better model prediction performance, with RPD > 2 representing excellent model performance. The calculation formulas for each indicator are as follows:

Correction set root mean square error:

$$RMSEC = \frac{\sqrt{\sum_{i=1}^{n}(h(x_i)-y_i)^2}}{n} \quad (2)$$

In the formula, $h(x_i)$ is the predicted value of the calibration set, y_i is the true value of the calibration set, and n is the number of samples in the calibration set.

Prediction set root mean square error:

$$RMSEP = \frac{\sqrt{\sum_{i=1}^{n}(h(x_i)-y_i)^2}}{n} \quad (3)$$

In the formula, $h(x_i)$ is the predicted value of the prediction set, y_i is the actual value of the prediction set, and n is the number of samples in the prediction set.

Adjusted correlation coefficient:

$$CCCS = \frac{\sum_{i=1}^{n}(x_i-\bar{x})(y_i-\bar{y})}{\sqrt{\sum_{i=1}^{n}(x_i-\bar{x})^2}-\sqrt{\sum_{i=1}^{n}(y_i-\bar{y})^2}} \quad (4)$$

In the formula, x_i is the predicted value of the calibration set, x is the mean predicted value of the calibration set, y_i is the actual value of the calibration set, y is the mean actual value of the calibration set, and n is the number of samples in the calibration set.

Prediction set correlation coefficient:

$$CCPS = \frac{\sum_{i=1}^{n}(x_i-\bar{x})(y_i-\bar{y})}{\sqrt{\sum_{i=1}^{n}(x_i-\bar{x})^2}-\sqrt{\sum_{i=1}^{n}(y_i-\bar{y})^2}} \quad (5)$$

In the formula, x_i is the predicted value of the prediction set, x is the mean of the predicted values of the prediction set, y_i is the actual value of the prediction set, y is the mean of the actual values of the prediction set, and n is the number of samples in the prediction set.

Correction set relative analysis error:

$$RPD = \frac{stdev}{rmse} \quad (6)$$

In the formula, stdev is the standard deviation of the calibration set samples, and rmse is the root mean square error of the calibration set samples.

The performance of partial least squares (PLS) models using different preprocessing methods is shown in Table 2.

Table 2. PLS Model Performance with Different Preprocessing

Preprocessing	Errata		Prediction set	
	R_C	RMSEC	R_P	RMSEP
Raw Spectrum	0.985	0.025	0.81	0.097
S-G	0.962	0.039	0.825	0.107
SVN	0.995	0.021	0.882	0.073
MSC	0.994	0.016	0.842	0.078

The results show that different preprocessing methods all have certain effects. Using spectra preprocessed by standard normal variate (SNV) transformation to establish a PLS prediction model, the correlation coefficients for the calibration set and validation set (RC and RP) were 0.989 and 0.882, respectively. The study results indicate that it is feasible to use hyperspectral imaging technology to predict the hardness of strawberries.

3.3. Detection of Soluble Solids in Strawberries

The reflectance spectra of strawberries extracted from hyperspectral images in the wavelength range of 400-1000 nm, where these bands reflect information about the physical parameters and biochemical characteristics of strawberries. In the visible light region, the absorption band near 680 nm may be related to chlorophyll [4], while the absorption band near 750 nm is attributed to the third

overtone of water [39]; in the near-infrared region, the absorption band near 960 nm is caused by the O-H of water [36]. The reflectance spectra of strawberries with different SSC and pH values show that in the 750-950 nm range, as SSC increases, the spectral reflectance also increases; in contrast, the spectral trend for pH is opposite, with spectral reflectance gradually decreasing as pH increases. In addition, for SSC and pH, the spectral changes in the 400-750 nm range are inconsistent with those in the 750-950 nm range, showing partial overlap in this region. In other words, the spectra of strawberries vary depending on their SSC and pH values. This phenomenon preliminarily demonstrates the feasibility of using HSI-extracted reflectance spectra to detect SSC and pH in strawberries.

4. SUMMARY

This study utilizes visible to near-infrared hyperspectral reflectance imaging technology (400-1000 nm) for detecting strawberry hardness, SSC, and pH. Hyperspectral imaging technology combines the advantages of spectroscopy and machine vision, allowing for both spectral features and image features such as color and texture to be extracted from hyperspectral images. Currently, there are very few studies using HSI for strawberry storage time or combining spectral and image features for SSC and pH detection. In this study, storage time is analyzed based on spectral features, while SSC and pH are analyzed using a combination of spectral, color, and texture features, and finally, the trends of SSC and pH changes over storage time are investigated. Compared with traditional conventional detection methods, the entire detection process is faster and more accurate, providing a novel method for non-destructive quality detection of strawberries and other fruits. This study not only offers a more efficient and convenient tool for practical strawberry quality detection but also provides a reference for future related research.

Overall, hyperspectral imaging technology shows great potential in the field of strawberry quality assessment, especially in detecting quality indicators such as SSC, acidity, hardness, and ripeness. This technology can effectively identify and classify the maturity levels of strawberries, predict their SSC, acidity, and hardness, providing a scientific basis for harvesting and grading. Although there are some technical and practical challenges, with the development of related technologies, hyperspectral imaging will gradually be more widely applied to the quality detection of strawberries and other agricultural products, offering solid technical support for agricultural production and food safety.

CONFLICTS OF INTEREST

The authors declare that they have no conflict of interest.

REFERENCES

[1] Li X, Wang D, Gong J, et al. Rapid and nondestructive detection of oil content and fatty acids of soybean using hyperspectral imaging[J]. Journal of Food Composition and Analysis,2025,139107033-107033.

[2] Huang P, Yang P, Xu L , et al. Moisture content detection of Tibetan tea based on hyperspectral technology, machine vision and machine learning[J].Journal of Food Measurement and Characterization, 2024 , (prepublish) :1-19.

[3] Mavroforakis M E, Theodoridis S. A geometric approach to support vector machine (SVM) classification[J]. IEEE transactions on neural networks, 2006, 17(3): 671-682.

[4] Zhu J, Ji G, Chen B, et al. High-throughput near-infrared spectroscopy for detection of major components and quality grading of peas[J]. Frontiers in Nutrition,2024,111505407-1505407.

[5] Mishra P, Nordon A, Mohd Asaari M S, et al. Fusing spectral and textural information in near-infrared hyperspectral imaging to improve green tea classification modelling[J]. Journal of Food Engineering, 2019, 249:40-47.

[6] Haralick R. Textural features for image classification[J]. IEEE Transactions on systems, man, and cybernetics, 1973, 6:610-621.

[7] Vera W, George A H, Mogollón J , et al.Food fraud detection in Octopus mimus using hyperspectral imaging and machine learning techniques[J].Neural Computing and Applications,2024,(prepublish):1-13.

[8] Knauer U, Warnemünde S, Menz P, et al. Detection of Apple Proliferation Disease Using Hyperspectral Imaging and Machine Learning Techniques[J].Sensors,2024,24(23):7774-7774.

[9] Fan L L, Zhao J L, Xu X G, et al. Hyperspectral-based estimation of leaf nitrogen content in corn using optimal selection of multiple spectral variables[J]. Sensors, 2019, 19(13):2898.

[10] Xu Y, Dong Y, Liu J , et al. Combination of near infrared spectroscopy with characteristic interval selection for rapid detection of rice protein content[J].Journal of Food Composition and Analysis,2025,137 (PB):106995.

[11] Lin Y, Fan R, Wu Y , et al. Combining hyperspectral imaging technology and visible-near infrared spectroscopy with a data fusion strategy for the detection of soluble solids content in apples[J].Journal of Food Composition and Analysis,2025,137(PB):106996-106996.

[12] Kasampalis S D, Tsouvaltzis I P, Siomos S A. Non-Destructive Detection of Pesticide-Treated Baby Leaf Lettuce During Production and Post-Harvest Storage Using Visible and Near-Infrared Spectroscopy [J]. Sensors, 2024, 24 (23): 7547.

[13] Michael M, Mariana B, Mirco B, et al. Field-level crop yield estimation with PRISMA and Sentinel-2[J]. ISPRS Journal of Photogrammetry and Remote Sensing, 2022, 187(2):191-210.

[14] Gila M M D, Martínez B D, Martínez S S , et al. Non-invasive detection of pesticide residues in freshly harvested olives using hyperspectral imaging technology[J]. Smart Agricultural Technology,2024,9100644-100644.

[15] He Q, Liu Z, Li X , et al.Detection of the Pigment Distribution of Stacked Matcha During Processing Based on Hyperspectral Imaging Technology[J].Agriculture,2024,14(11):2033-2033.

[16] Xianghai C, Da W, Xiaozhen W, et al. Hyperspectral imagery classification with cascaded support vector machines and multi-scale superpixel segmentation[J]. International Journal of Remote Sensing, 2020, 41(12):4530-4550.

[17] Fan L L, Zhao J L, Xu X G, et al. Hyperspectral-based estimation of leaf nitrogen content in corn using optimal selection of multiple spectral variables[J]. Sensors, 2019, 19(13):2898.

[18] Erdinç S, Yaşar K, Oğuz Ö, et al. Estimating technological quality parameters of bread wheat using sensor-based Normalized Difference Vegetation Index[J]. Journal of Cereal Science, 2022, 107(8).

[19] Wang Q, Lu J, Wang Y, et al. Research on Nondestructive Inspection of Fruits Based on Spectroscopy Techniques: Experimental Scenarios, ROI, Number of Samples, and Number of Features[J].Agriculture,2024,14(7):977-977.

[20] Assi S, Abbas I, Tang L , et al. Evaluating the detection of cocaine and its impurities concealed inside fruit- and vegetable- food products using handheld spatially offset Raman spectroscopy[J].Vibrational Spectroscopy, 2024, 131103662-.

[21] Zhang B, Huang W, Li J, et al. Principles, developments and applications of computer vision for external quality inspection of fruits and vegetables: A review[J]. Food Research International, 2014, 62: 326-343.

[22] Zhuang X, Xiang Y, Qiang H, et al. Quality analysis of olive oil and quantification detection of adulteration in olive oil by near-infrared spectrometry and chemometrics[J]. Spectroscopy and Spectral Analysis, 2010, 30(4): 933-936.

[23] Li H, Liang Y, Xu Q, et al. Key wavelengths screening using competitive adaptive reweighted sampling method for multivariate calibration[J]. Analytica chimica acta, 2009, 648(1): 77-84.

[24] Hui G Y, Sun L J, Wang J N, et al. Research on the pre-processing methods of wheat hardness prediction model based on visible-near infrared spectroscopy[J]. Spectroscopy and Spectral Analysis, 2016, 36(7): 2111-2116.

[25] Yang Y, Zhuang H, Yoon S C, et al. Rapid classification of intact chicken breast fillets by predicting principal component score of quality traits with visible/near-infrared spectroscopy[J]. Food chemistry, 2018, 244: 184-189.

[26] Rogel-Castillo C, Boulton R, Opastpongkarn A, et al. Use of near-infrared spectroscopy and chemometrics for the nondestructive identification of concealed damage in raw almonds (Prunus dulcis)[J]. Journal of agricultural and food chemistry, 2016, 64(29): 5958- 5962.

[27] Wiedemair V, Ramoner R, Huck C W. Investigations into the total antioxidant capacities of cultivars of gluten-free grains using near-infrared spectroscopy[J]. Food control, 2019, 95: 189-195.

[28] Melenteva A, Galyanin V, Savenkova E, et al. Building global models for fat and total protein content in raw milk based on historical spectroscopic data in the visible and short- wave near infrared range[J]. Food chemistry, 2016, 203: 190-198.

[29] Sun T, Lin H, Xu H, et al. Effect of fruit moving speed on predicting soluble solids content of ‘Cuiguan’ pears (Pomaceae pyrifolia Nakai cv. Cuiguan) using PLS and LS-SVM regression[J]. Postharvest biology and technology, 2009, 51(1): 86-90.

[30] Weng S, Yu S, Guo B, et al. Non-Destructive Detection of Strawberry Quality Using Multi-Features of Hyperspectral Imaging and Multivariate Methods[J]. Sensors, 2020, 20(11):3074.

[31] Diago M P, Fernandez-Novales J, Fernandes AM, et al. Use of visible and short-wave near- infrared hyperspectral imaging to fingerprint anthocyanins in intact grape berries[J]. Journal of agricultural and food chemistry, 2016, 64(40): 7658-7666.

[32] Li B, Cobo-Medina M, Lecourt J, et al. Application of hyperspectral imaging for nondestructive measurement of plum quality attributes[J]. Postharvest Biology and Technology, 2018, 141: 8-15.

[33] Kizilboga Y A, ErgÃ¼zen A, Erdal E. Determination of Various Diseases in Two Most Consumed Fruits using Artificial Neural Networks and Deep Learning Techniques[J].Journal of Trend in Scientific Research and Development, 2020,5(1):

[34] Manuela M, Luca M ,Elena L , et al. Application of Near Infrared Spectroscopy for the Rapid Assessment of Nutritional Quality of Different Strawberry Cultivars.[J].Foods (Basel, Switzerland),2023,12(17):

[35] Jeremy W, Arjun N, Anand K , et al. Review: The evolution of chemometrics coupled with near infrared spectroscopy for fruit quality evaluation. II. The rise of convolutional neural networks[J].Journal of Near Infrared Spectroscopy, 2023, 31(3):109-125.

[36] Weixin Y, Wei X, Tianying Y, et al. Application of Near-Infrared Spectroscopy and Hyperspectral Imaging Combined with Machine Learning Algorithms for Quality Inspection of Grape: A Review[J]. Foods,2022,12(1):132-132.

[37] Li L, Yuan D H, Yu T T , et al.Non-destructive detection of the quality attributes of fruits by visible-near infrared spectroscopy[J].Journal of Food Measurement and Characterization,2022,17(2):1526-1534.

[38] Syed S A S, Ayesha Z, Waqar S, et al. Towards Fruit Maturity Estimation Using NIR Spectroscopy[J].Infrared Physics & Technology,2020,111(prepublish):103479-.

[39] Alex G, Sara S, Stefano M. Postharvest Dry Matter and Soluble Solids Content Prediction in d' Anjou and Bartlett Pear Using Near-infrared Spectroscopy[J]. HortScience,2018,53(5):669-680.

[40] Peilong X. Research and application of near-infrared spectroscopy in rapid detection of water pollution[J]. DESALINATION AND WATER TREATMENT,2018,1221-4.

[41] Nagata M, Tallada J G, Kobayashi T, et al. Predicting maturity quality parameters of strawberries using hyperspectral imaging[A]. 2004 ASAE Annual Meeting[C]. American Society of Agricultural and Biological Engineers, 2004, 1.

[42] Ding X B, Zhang C, Liu F, et al. Determination of soluble solid content in strawberry using hyperspectral imaging combined with feature extraction methods[J]. Spectroscopy and Spectral Analysis, 2015, 35(4): 1020-1024.

[43] Yeh Y H, Chung W C, Liao J Y, et al. Strawberry foliar anthracnose assessment by hyperspectral imaging[J]. Computers and Electronics in Agriculture, 2016, 122: 1-9.

[44] Liu Q, Wei K, Xiao H, et al. Near-infrared hyperspectral imaging rapidly detects the decay of postharvest strawberry based on water-soluble sugar analysis[J]. Food Analytical Methods, 2019, 12(4): 936-946.

[45] Nagata M, Tallada J G, Kobayashi T, et al. NIR hyperspectral imaging for measurement of internal quality in strawberries[A]. 2005 ASAE Annual Meeting[C]. American Society of Agricultural and Biological Engineers, 2005, 1.

[46] Moreno R, Corona F, Lendasse A, et al. Extreme learning machines for soybean classification in remote sensing hyperspectral images[J]. Neurocomputing, 2014, 128: 207- 216.

[47] Ding H, Chang R C. Comparison of photometric stereo and spectral analysis for visualization and assessment of burn injury from hyperspectral imaging[A]. 2015 IEEE International Conference on Computational Intelligence and Virtual Environments for Measurement Systems and Applications (CIVEMSA)[C]. IEEE, 2015, 1-6.

[48] Zhang Y, Guo W. Moisture content detection of maize seed based on visible/near -infrared and near -infrared hyperspectral imaging technology[J]. International Journal of Food Science & Technology, 2020, 55: 631-640.

[49] Zhao Y, Zhang C, Zhu S, et al. Shape induced reflectance correction for non-destructive determination and visualization of soluble solids content in winter jujubes using hyperspectral imaging in two different spectral ranges [J]. Postharvest Biology and Technology, 2020, 161: 111080.

[50] Saptoro A, Tadé M O, Vuthaluru H. A modified Kennard-Stone algorithm for optimal division of data for developing artificial neural network models[J]. Chemical Product and Process Modeling, 2012, 7(1): 1-16.

[51] Zou X, Shi J, Hao L, et al. In vivo noninvasive detection of chlorophyll distribution in cucumber (Cucumis sativus) leaves by indices based on hyperspectral imaging[J]. Analytica Chimica Acta, 2011, 706(1): 105-112.

[52] Viña S Z, Chaves A R. Effect of heat treatment and refrigerated storage on antioxidant properties of pre -cut celery (Apium graveolens L.) [J]. International journal of food science & technology, 2008, 43(1): 44-51.

[53] Yan L, Xiong C, Qu H, et al. Non-destructive determination and visualisation of insoluble and soluble dietary fibre contents in fresh-cut celeries during storage periods using hyperspectral imaging technique[J]. Food Chemistry, 2017, 228: 249-256.

[54] Ma J, Sun D W, Pu H. Spectral absorption index in hyperspectral image analysis for predicting moisture contents in pork longissimus dorsi muscles[J]. Food chemistry, 2016, 197: 848-854.